






Article

Expanding the Application Range of Microbial Oxidoreductases by an Alcohol Dehydrogenase from *Comamonas testosteroni* with a Broad Substrate Spectrum and pH Profile

Daniel Bakonyi ^{1,†,§}, Christine Toelzer ^{2,‡,§}, Michael Stricker ¹, Werner Hummel ¹,
Karsten Niefind ^{2,*} and Harald Gröger ^{1,*}

¹ Industrial Organic Chemistry and Biotechnology, Faculty of Chemistry, Bielefeld University, Universitätsstr. 25, D-33615 Bielefeld, Germany; Daniel.Bakonyi@ime.fraunhofer.de (D.B.); michael.stricker@uni-bielefeld.de (M.S.); w.hummel@fz-juelich.de (W.H.)

² Institute of Biochemistry, Department of Chemistry, University of Cologne, Zùlpicher Str. 47, D-50674 Cologne, Germany; christine.toelzer@bristol.ac.uk

* Correspondence: karsten.niefind@uni-koeln.de (K.N.); harald.groeger@uni-bielefeld.de (H.G.)

† Current Address: Fraunhofer Institute for Molecular Biology and Applied Ecology (IME), Project Group Bioresources, Ohlebergsweg 12, D-35392 Giessen, Germany.

‡ Current Address: Bristol Synthetic Biology Centre BrisSynBio, Biomedical Sciences, School of Biochemistry, University of Bristol, BS8 1TD Bristol, UK.

§ These authors contributed equally to this work.

Received: 4 October 2020; Accepted: 29 October 2020; Published: 4 November 2020



Abstract: Alcohol dehydrogenases catalyse the conversion of a large variety of ketone substrates to the corresponding chiral products. Due to their high regio- and stereospecificity, they are key components in a wide range of industrial applications. A novel alcohol dehydrogenase from *Comamonas testosteroni* (CtADH) was identified in silico, recombinantly expressed and purified, enzymatically and biochemically investigated as well as structurally characterized. These studies revealed a broad pH profile and an extended substrate spectrum with the highest activity for compounds containing halogens as substituents and a moderate activity for bulky–bulky ketones. Biotransformations with selected ketones—performed with a coupled regeneration system for the co-substrate NADPH—resulted in conversions of more than 99% with all tested substrates and with excellent enantioselectivity for the corresponding *S*-alcohol products. CtADH/NADPH/substrate complexes modelled on the basis of crystal structures of CtADH and its closest homologue suggested preliminary hints to rationalize the enzyme’s substrate preferences.

Keywords: alcohol dehydrogenase; asymmetric synthesis; biotransformation; protein crystallography; protein structure; short chain dehydrogenase/reductase

1. Introduction

Oxidoreductases have a wide substrate scope and can act on organic substrates including alcohols, ketones/aldehydes, amines and inorganic substrates including small ions such as sulphite [1–4]. Therefore, they are a valuable class of enzymes to synthesize complex chiral products under mild reaction conditions and with high chemo-, regio- and stereoselectivity [5,6]. The resulting enantiomerically pure chemicals are essential chiral building blocks for the production of chiral pharmaceuticals, drugs or flavours [7,8].

NAD(P)(H)-dependent alcohol dehydrogenases (ADHs) represent one of the largest groups of biotechnologically applied oxidoreductases. In particular, the so-called short-chain reductases/

dehydrogenases (SDR) which are spread among all kingdoms of life [9] provide a large fund of valuable biocatalysts. The application range of SDR enzymes and other ADHs has been enlarged in recent years by several promising efforts:

- (i) ADHs require nicotinamide cofactors—NAD(H) or NADP(H)—to perform their function. These compounds (in particular NADP⁺ and NADPH) are expensive, which can be a limiting factor for industrial biocatalysis. A modern solution of the problem is the application of an integrated efficient recycling system that allows process operation under economic conditions. For this purpose, two cofactor regeneration systems—enzyme-coupled and substrate-coupled—have been developed and described in detail [10–12]. Furthermore, the co-substrate specificity might be changed from NADP(H)- to NAD(H) dependence by site-directed mutagenesis, which then allows the utilization of the less expensive cofactor NAD(H) [13].
- (ii) Several ADHs are comparatively pH- and thermostable [14,15], robust against stress imposed by non-aqueous solvents [16] and can be optimized in these directions. Thermostable and solvent-resistant enzymes are particularly valuable if hydrophobic substrates with solubility problems in aqueous media are processed [17].
- (iii) The spectrum of substrates accepted by ADHs is rather broad ranging—for example, from small alcohols such as isopropanol [18] via sugars [12] to complex steroids [19,20]—and is often accompanied by a significant and synthetically attractive enantioselectivity. Accordingly, in case an important reaction step in asymmetric synthesis is accomplished, rather than mutating a well-known ADH, it is often more promising to screen for a novel ADH activity with the required profile [1]. With the growing number of annotated but not further characterized ADHs revealed by genome sequencing, it becomes increasingly attractive to perform such screening efforts in silico [21].

The enzymatic production of chiral secondary alcohols from asymmetric ketones is a particularly important and ambitious task. Many ADHs for the transformation of “small-bulky” ketones were described in the past [13,22], whereas ADHs accepting “bulky-bulky” ketones are much less abundant. Two enzymes with this profile were found in *Ralstonia* sp. DSM 6428 (RasADH) [23,24] and in *Sphingobium yanoikuyae* DSM 6900 (SyADH) [25]; both enzymes have been structurally characterized in a complex with NADPH [26].

In this study, we supplement this collection with an ADH from *Comamonas testosteroni* (CtADH). *Comamonas testosteroni* belongs to the betaproteobacteria, which have versatile metabolic capacities and possess a wide spectrum of substrate utilization [27]. Its complete genome is sequenced and available [28,29]. The rationale to choose *C. testosteroni* as source of a novel ADH with valuable properties was its occurrence in polluted environments and its ability to convert xenobiotics. Strains of *C. testosteroni* have been paid great attention due to their capability of utilizing testosterone and derivatives such as bile acids and other xenobiotic compounds [19,20,30–32]. For example, *C. testosteroni* CNB-1 has been successfully applied in environment bioremediation to degrade 4-chloronitrobenzene in soil [33].

We describe here the in silico identification, heterologous expression and biochemical characterization of CtADH. Kinetic and structural analysis were performed to develop a deeper understanding of the structure–activity relationship of this enzyme towards bulky–bulky as well as halogenated substrates. In addition, the impact of organic solvents on the stability of CtADH and a pH profile of the catalytic activity are explored.

2. Results and Discussion

2.1. Identification of the Alcohol Dehydrogenase Gene

In GenBank [34] (entry WP_003056551.1), CtADH is classified as a putative short-chain dehydrogenase/reductase (SDR). The gene comprises 789 bp and encodes 262 amino acids. The closest homologue of CtADH with known 3D-structure (sequence identity 77%) and thus representing a

reference enzyme is SyADH. A sequence alignment with SyADH and other related ADHs (Figure 1) confirms the classification of CtADH as a member of the SDR family and encompasses the typical Rossmann fold with the glycine motif at the N-terminus and conserved catalytic triad residues.

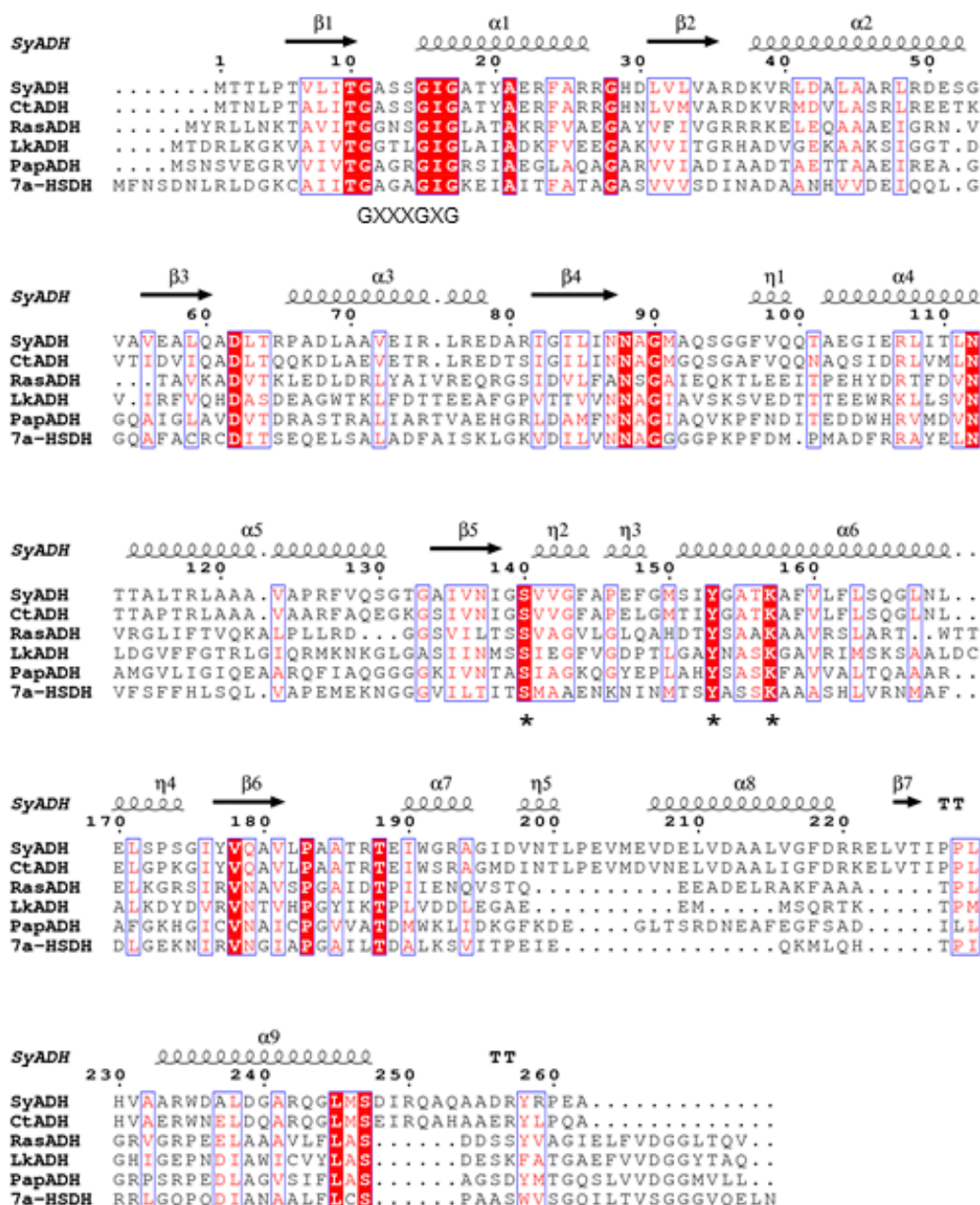


Figure 1. Multiple sequence alignment of CtADH, SyADH (genbank: EU427523.1), PapADH (EU427522.1), RasADH (ACB78191.1), LkADH (AY267012.1) and 7α-HSDH (AJP09756.1), illustrated with ENDscript [35] including structural information from SyADH [26]. Secondary structure elements are presented on top: helices with squiggles, beta strands with arrows and turns with TT letters. Positions with high similarity are boxed in blue and written in red; absolutely conserved regions are boxed in red. The glycine-motif GXXXGXXG is indicated as described and the amino acid residues of the catalytic triad are marked with a star.

2.2. Cloning and Heterologous Overexpression of CtADH

Standard cloning techniques were used to create the recombinant plasmid pET28a_CtADH(C) with a hexahistidine affinity purification motif (His-tag), fused to the C-terminus of the protein.

The recombinant plasmid was expressed in *E. coli* BL21(DE3) at different temperatures and media, revealing the best expression in TB medium at 25 °C (Figure S1a). The crude and purified enzymes were analysed by SDS-PAGE (Figure S1b). The over-expressed CtADH was clearly displayed (Figure S1a). The band was estimated at about 25 kDa, which is in good accordance with the calculated molecular weight of 29.7 kDa. Already in the crude extract, the high over-expression of this enzyme could be demonstrated (Figure S1b).

2.3. Substrate Specificity, Kinetic Parameters and Enantioselectivity of CtADH

The activity of CtADH in reduction direction was studied with linear aliphatic, aromatic ketones, halogenated and “bulky-bulky” compounds (Table 1) and the oxidation with a variety of alcohols (Table 2). The substrate specificity of the enzyme was determined by spectrophotometric assays for both reaction directions.

In general, CtADH showed a very broad substrate range as figured in Table 1. The highest activity was obtained with 2,2,2-trifluoroacetophenone (entry 12, 127.7 U mg⁻¹) and 2,3-pentandione (entry 15, 85.9 U mg⁻¹). Many other aliphatic compounds were also converted such as 2-heptanone and 4-nonanone. In addition, halogenated, cyclic and even “bulky-bulky” compounds turned out to be suitable substrates and were converted with, at least in part, high activities. Reductions of halogenated compounds are of importance because those substrates are often intermediates in the synthesis of active pharmaceutical ingredients (APIs) [36,37]. Furthermore, “bulky-bulky” substrates, such as ethyl benzoylformate, are well accepted with an especially high activity in this case (entry 10, 82.9 U mg⁻¹). “Bulky-bulky” ketones with both bulky substituents (larger than ethyl) to the carbonyl carbon are challenging to be reduced by most ADHs due to the size limitation of the small binding pocket.

Table 1. Spectrophotometrically determined activities for the reduction of various ketone substrates by CtADH. The activities were obtained by use of the standard spectrophotometric assay. (* marks the chiral center of the product.)

$$\text{R}-\overset{\text{O}}{\parallel}{\text{C}}-\text{R}' \xrightarrow[\text{NADPH} \rightarrow \text{NADP}^+]{\text{ADH from } \textit{Comamonas\ testosteroni} \text{ (overexpressed in } \textit{E. coli})}} \text{R}-\overset{\text{OH}}{\underset{*}{\text{C}}}-\text{R}'$$

#	Substrate	Concentration [mM]	Spec. Activity [U mg ⁻¹]
1	2-aminoacetophenone hydrochloride	50	0.1
2	4-phenyl-2-butanone	10	8.1
3	ethyl 2-oxo-4-phenylbutyrate	10	0.4
4	4-chlorobutyrophenone	<10	3.7
5	acetophenone	10	0.8
6	propiophenone	10	1.4
7	(R)-carvone	<10	0.5
8	ethyl 4-chloroacetoacetate	10	3.4
9	cyclohexanone	10	1.2
10	ethyl benzoylformate	1	82.9
11	ethyl acetoacetate	50	18.5
12	2,2,2-trifluoroacetophenone	10	127.7
13	4-hydroxy-2-butanone	50	0.3
14	2-heptanone	10	6.1
15	2,3-pentandione	50	85.9
16	4-nonanone	<10	2.8
17	2-octanone	<10	5.6
18	ethyl 4,4,4-trifluoroacetoacetate	50	4.6
19	2-chlorocyclopentanone	25	12.1
20	2-chlorocyclohexanone	25	64.2

Table 2. Spectrophotometrically determined activities for the oxidation of various alcohol substrates by CtADH. The activities were obtained by use of the standard spectrophotometric assay with a substrate concentration of 10 mM in all cases. (* marks the chiral center of the product.)

#	Substrate	Spec. Activity [U mg ⁻¹]
21	4-phenyl-2-butanol	3.4
22	<i>rac</i> -1-phenylethanol	1.0
23	(<i>R</i>)-1-phenylethanol	0.1
24	(<i>S</i>)-1-phenylethanol	0.7
25	<i>rac</i> -1-phenylpropanol	1.0

For the direction of the oxidation, only aromatic substrates were tested (Table 2). The best activity was obtained with 4-phenyl-2-butanol (entry 21, 3.4 U mg⁻¹). Further investigation of the oxidative reaction is necessary to gain accurate information regarding the substrate profile.

The kinetic parameters of the purified CtADH for the substrate propiophenone (reduction) and (*S*)-1-phenylethanol (oxidation), together with the cofactor NADPH and NADP⁺, respectively, were measured at 27.5 (reduction) and 28.8 °C (oxidation) at pH 6, respectively (Figure S2). For propiophenone, the Michaelis–Menten constant (K_M) was determined to be 0.62 ± 0.07 mM and the maximum specific velocity (V_{max}) was 0.53 ± 0.02 U mg⁻¹ (Figure S2a). For the oxidative reaction with (*S*)-1-phenylethanol, the Michaelis–Menten constant (K_M) was determined to be 1.72 ± 0.05 mM and the maximum specific velocity (V_{max}) was 0.21 ± 0.01 U mg⁻¹ (Figure S2b). For the cofactor NADPH, together with 1 mM propiophenone, the determined kinetic constants were $K_M = 13.9 \pm 1.1$ μM and $V_{max} = 0.39 \pm 0.01$ U mg⁻¹ (Figure S2c).

The asymmetric reduction of ketones to their corresponding alcohols in the presence of CtADH as biocatalyst were performed in a monophasic aqueous system and compared to the biotransformations with the recombinant SyADH (Table 3).

Table 3. Reduction of selected ketones by CtADH and SyADH. Degrees of conversion and ee values were determined by chiral GC. (* marks the chiral center of the product.)

Substrate	CtADH		SyADH	
	Conversion [%]	Selectivity [ee]	Conversion [%]	Selectivity [ee]
acetophenone	>99	(<i>S</i>) 97%	>99	(<i>S</i>) 98%
ethyl benzoylformate	>99	(<i>S</i>) 65%	>99	(<i>S</i>) 57%
ethyl 4-chloroacetoacetate	>99	(<i>S</i>) 96%	>99	(<i>R</i>) 41%
4-chlorobutyrophenone	>99	(<i>S</i>) 99%	>99	(<i>S</i>) 99%
2,2,2-trifluoroacetophenone	>99	(<i>S</i>) 77%	>99	(<i>S</i>) 58%
ethyl 4,4,4-trifluoroacetoacetate	>99	(<i>S</i>) 99%	>99	(<i>S</i>) 83%

All tested substrates were reduced to the corresponding (*S*)-alcohols with high enantioselectivity (over 96% *ee*) except for ethyl benzoylformate and 2,2,2-trifluoroacetophenone, which were reduced with an enantioselectivity of 65% and 77% *ee*, respectively. This result indicates that CtADH is an (*S*)-specific ADH. It is noteworthy that in comparison, the SyADH showed a decreased enantioselectivity for most of the tested substrates. The ketone ethyl 4-chloroacetoacetate was even converted to the (*R*)-enantiomer with 41% *ee*. According to these results, CtADH appears to be a promising catalyst candidate for biotransformations of a broad range of diverse substrates with high enantioselectivity. Future experiments will serve to explore if the attractive combination of high selectivity and conversion holds true at higher substrate concentrations as well.

2.4. pH-Profile of Catalytic Activity and Effect of Organic Solvents on CtADH Stability

To test the dependence of CtADH activity on the pH-value and organic solvents, the reduction of propiophenone was measured under various conditions. For the determination of the pH optimum, three buffers with overlapping pH ranges were used (citrate acid/phosphate buffer (pH 4.5 to 7.5), Tris/HCl buffer (pH 8.0 to 9.0) and bicine buffer (pH 8.0 to 12.1)) (Table S2). The enzyme showed a good activity (>90%) over a broad pH range from pH 5.5 to 8.5 (Figure 2a). This correlates well with the fact that the melting point of CtADH exceeds 40 °C in most applied buffers except those at pH 5 or lower (Figure S3). The activity optimum was determined to be at pH 7.0 in citrate acid/phosphate buffer (Figure 2a). This broad pH range of the reduction reaction represents an advantage when using CtADH as a biocatalyst.

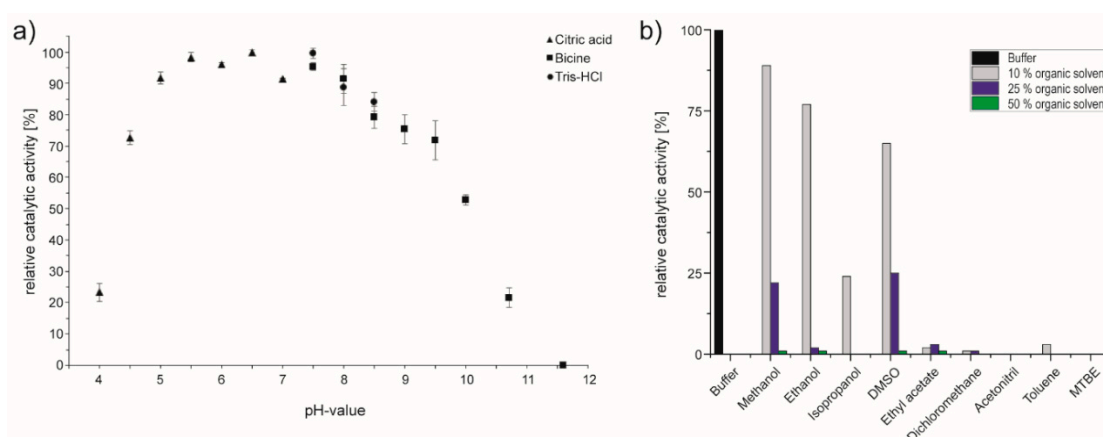


Figure 2. Ambient solution effects on the activity and stability of purified CtADH. The activity of CtADH was measured with 0.1 M propiophenone as substrate and 0.2 mM NADPH as co-substrate. (a) pH-profile of the catalytic activity of CtADH determined with three different buffer systems (Table S2). (b) Effect of preincubation in organic solvents at different solvent concentrations on the stability of CtADH assayed by the reduction of propiophenone. The grey bars indicate the activities when using 10% (*v/v*) organic solvent, cyan bars correspond to the activities when using 25% (*v/v*) of organic solvent and green bars correspond to the activities measured at 50% (*v/v*) of organic solvent.

To overcome the drawbacks of low solubility of many organic substrates in “conventional” aqueous phase, the addition of organic solvents to the biocatalytic systems is a promising approach to improve the productivity [38]. However, organic solvents frequently decrease enzyme stability [39]. Therefore, we studied the stability of CtADH in water miscible and immiscible common organic solvents. As shown in Figure 2b, after incubation in different organic solvent/buffer systems for 2 h at 25 °C, the CtADH turned out to be remarkably stable in the presence of methanol, ethanol and DMSO when being used in an amount of 10% (*v/v*). In contrast, in the presence of water-immiscible organic solvents, only a low activity could be measured when using ethyl acetate, dichloromethane and toluene as solvent components.

2.5. Structural Characterization of CtADH

Extensive crystallization efforts with CtADH led to an orthorhombic and a tetragonal crystal form. The crystals X-rays to resolutions of about 2.0 Å and 2.2 Å and led to structures of acceptable quality (Table S1) comprising three (orthorhombic structure) or two (tetragonal structure) crystallographically independent CtADH protomers per asymmetric unit.

The structures contain the apo-form of CtADH without any substrate or co-substrate ligands despite the presence of such compounds in the crystallization drops. This deficit may contribute to the fact that in all five CtADH monomers, a functionally critical part—the helical $\alpha 5/\eta 7$ region that covers the active site in a catalytically fully competent enzyme/substrate complex—is disordered and not defined by electron density (Figure 3a). Otherwise, the tertiary structure of CtADH shows the typical open α/β topology of SDR enzymes based on a classical Rossmann fold: a central seven-stranded parallel β -sheet to which eight α -helices of different lengths are attached on both sides (Figure 3a). Two of these helices ($\alpha 4$ and $\alpha 5$) seamlessly merge into each other (Figure 1).

Like SyADH, CtADH contains a non-canonical helix $\alpha 9$ in its C-terminal segment (Figure 3a). This helix sticks out from the main domain since it has a special double role at the level of the quaternary structure: as typical for SDR enzymes, the large helices $\alpha 4/\alpha 5$ and $\alpha 6$ function as a dimerization module and form a four-helix bundle with a second CtADH monomer (Figure 3b); yet, in contrast to most SDR enzymes (but similar to SyADH), the particular helix $\alpha 9$ crosses over to the second subunit and forms a helical pair with its counterpart within the dimer. In this way, the helix $\alpha 9$ stabilizes the dimeric architecture (Figure 3b); simultaneously, however, it blocks the surface used by the majority of SDR enzymes to coordinate a second dimer and thus to establish a homotetramer with D2 point symmetry. In Figure 3b, this is illustrated with the *R*-specific alcohol dehydrogenase from *Lactobacillus brevis* (LbRADH) [13,22] which accordingly contains a much shorter C-terminal segment (Figure 3a).

To rationalize the essentials of CtADH's substrate and stereospecificity, we modelled a ternary complex of the enzyme with the substrate *n*-pentyl phenyl ketone and the co-substrate NADPH in silico (Figure 3a). To this end, we took over NADPH from its binary complex structure with SyADH (PDB-ID 4BMV); with respect to the substrate, we adapted the modelling strategy described for the SyADH/NADPH/*n*-pentyl phenyl ketone complex [26]. In a plausible catalytic complex, the carbonyl group of the ketonic substrate must be properly located and oriented relative to the co-substrate NADPH and to the catalytic key residues Ser140 and Tyr153. Therefore, the substrate molecule was modelled in such a way into a kind of substrate-binding tunnel that the carbonyl O-atom is in hydrogen bonding distance to the side chains of Ser140 and Tyr153 and that the carbonyl C-atom is close enough to the C4-atom of the nicotinamide ring to allow hydride transfer (Figure 3a,b).

Further, similar to what had been done for SyADH [26], we placed *n*-pentyl phenyl ketone such that its re-plane faces NADPH. This orientation, in which the phenyl ring is embedded in a hydrophobic environment within the outer part of the substrate-binding tunnel formed by Val141, Leu148, Ala184/185 and Trp191 (Figure 3a), would lead to the product *S*-1-phenyl hexanol and is thus consistent with the preference of CtADH for the (*S*)-enantiomer of 1-phenyl ethanol, a CtADH substrate in oxidation direction (Table 2). *R*-1-phenyl ethanol, however, is oxidized under CtADH catalysis as well, albeit with a significantly lower specific activity (Table 2). Thus, CtADH prefers to accommodate a bulky phenyl substituent in the outer substrate binding tunnel as indicated in Figure 3c,d, but can essentially place it alternatively as well, namely at the inner region of the tunnel occupied by the *n*-propyl chain in Figure 3c,d. This spaciousness at both sides of the tunnel fits to the bulky–bulky substrate profile of CtADH indicated among others by the fact that propiophenone is a better substrate than acetophenone (Table 1). In contrast, in an enzyme such as LbRADH that prefers acetophenone and other small-bulky ketones as substrates [13,40], the space at the outer tunnel region is restricted by the side chains of Tyr189 and Ile143 (Figure 3d) which excludes the binding of a bulky moiety and forces ketonic substrates into an orientation that necessarily leads to (*R*)-alcohol products.

The example of LbRADH shows that the substrate profile and the stereospecificity can be strongly correlated. Accordingly, for bulky–bulky ADHs such as CtADH or SyADH with small spatial

limitations on both sides of the substrate-binding tunnel, one would expect only a low enantioselectivity. Interestingly (and most attractively for application purposes), however, this is not the case: the data set in Table 3 suggests that CtADH is even more enantioselective than SyADH and prefers the formation of the *S*-enantiomer of an alcoholic reaction product more strongly than the latter. If space restrictions such as in LbRADH are not sufficient to enforce this enantioselectivity, more subtle molecular interactions within the substrate-binding tunnel must exist that favour one specific orientation of a ketonic substrate over the other. Possibly, the two substitutions between CtADH and SyADH illustrated in Figure 3c (Leu148/Phe148 and Gly92/Ala92) are critical for the enhanced enantioselectivity of CtADH. Mutational studies and, in particular, experimental complex structures of the enzymes with substrates or significant inhibitors are required to allow a deeper rationalization of these connections.

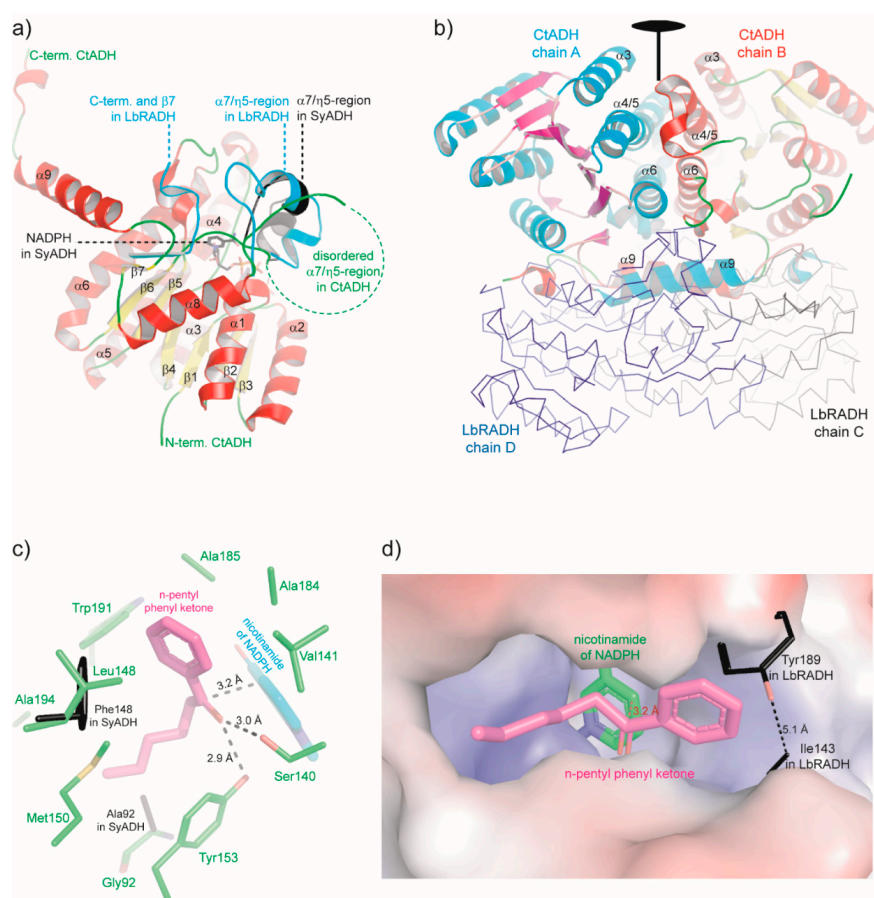


Figure 3. Structure of CtADH. (a) Overview of a CtADH monomer with secondary structure elements labelled according to the sequence alignment in Figure 1. For comparison, parts of the structures of the SyADH/NADPH complex (PDB-ID 4BMV [26]) and of apo-LbRADH (PDB-ID 1NXQ [22]) were depicted after structural overlay on CtADH. (b) Dimerization of CtADH via a central four-helix bundle ($\alpha 4/5$ plus $\alpha 6$), assisted by the non-canonical helices $\alpha 9$, from both subunits. To illustrate how the helix $\alpha 9$ couple blocks the tetramerization surface of typical tetrameric SDR enzymes, two subunits of the LbRADH tetramer [22] were drawn after superimposition of the other two subunits (not shown) on the CtADH dimer. (c) Active site region of an in silico model of CtADH in complex with NADPH and the substrate *n*-pentyl phenyl ketone. Two side chains of SyADH different from CtADH were drawn with black C-atoms after structural overlay of the proteins. (d) Substrate-binding tunnel of CtADH occupied with *n*-pentyl phenyl ketone (in silico model). To illustrate the generous space supply in the outer part of the substrate-binding tunnel of CtADH, two LbRADH side chains were drawn (black C-atoms) that restrict the space in this region of LbRADH significantly.

3. Materials and Methods

3.1. Origin of Chemicals

All used chemicals were of high analytical grade and purchased from Sigma Aldrich (Steinheim, Germany) and Carl Roth (Karlsruhe, Germany). Coenzymes were bought from Biomol (Hamburg, Germany). Ni-NTA resin was purchased from MCLAB (San Francisco, CA, USA) and restriction enzymes, Phusion™-Polymerase, Plasmid isolation kits as well as T4 ligase from ThermoScientific (Waltham, MA, USA). Oligonucleotids were synthesized by EurofinsMWG (Ebersberg, Germany).

3.2. Identification, Cloning and Heterologous Expression of CtADH and SyADH

The protein sequence of the “bulky-bulky” alcohol dehydrogenase SyADH (GenBank [34] entry EU427523) [17,26] was used as the query sequence for BLAST analysis [41] for the identification of potential alcohol dehydrogenase candidates. After analysis of the results, focusing on the *Comamonas* species, a gene from *Comamonas testosteroni* with a similarity of 77% was chosen as the gene of interest. This gene (GenBank: WP_003056551.1) was amplified from the *Comamonas testosteroni* strain DSM 38 via polymerase chain reaction (PCR), cloned into the pET28a plasmid and transformed into *Escherichia coli* BL21(DE3) (see supporting information).

For protein overexpression, TB auto induction medium, TB as well as LB medium were tested. Auto induction media containing 2 g L⁻¹ lactose, 0.5 g L⁻¹ glucose and 50 µg mL⁻¹ kanamycin were inoculated with 1% of an overnight preculture. The cells were incubated at 37 °C for 2 h and then for 72 h at 15 °C. TB and LB media with appropriate kanamycin were inoculated with 1% of an overnight preculture, and the induction of the gene was started by the addition of 500 µM isopropyl-β-D-thiogalactopyranoside (IPTG) when the OD₆₀₀ reached 0.4 to 0.6. Cells were harvested after 18 h at 25 °C for LB and TB media, and additionally at 30 or 37 °C for the TB media, and stored at -20 °C until further use.

The SyADH gene was chemically synthesized in codon-optimized form by GeneArt (ThermoFisher, Germany). A hexahistidine-tag was fused to the N-terminus and bacterial expression was performed equally to the one of the CtADH.

3.3. Purification of CtADH and SyADH

Purified protein was obtained by Ni-NTA immobilized metal affinity chromatography (IMAC). The column was equilibrated with 25 mL lysis buffer (10 mM imidazole, 300 mM NaCl, 50 mM NaH₂PO₄, pH 8.0). The cell lysate containing his-tag fusion protein was applied on the column and washed with 50 mL washing buffer (25 mM imidazole, 300 mM NaCl, 50 mM NaH₂PO₄, pH 8.0). The bound protein was eluted with 10 mL elution buffer (250 mM imidazole, 300 mM NaCl, 50 mM NaH₂PO₄, pH 8.0). After a desalting step with a PD10 column (Sephadex G25, GE healthcare, Munich, Germany), the enzyme was stored in 100 mM citrate-phosphate buffer pH 6.0 and kept at 4 °C until use.

For the purpose of crystallization, the CtADH purification was supplemented with an additional size exclusion step in 25 mM Hepes, 150 mM NaCl, pH 7.5.

3.4. Crystallization and Structure Determination of CtADH

CtADH crystals were grown by the vapour diffusion sitting drop method at 20 °C by mixing 1 µL of protein solution with 1 µL of reservoir solution. The optimized reservoir compositions providing crystals suitable for data collection were 20% (v/v) polyethylene glycol 1500; 0.1 M sodium-HEPES, pH 7.5, in case of the orthorhombic crystals; and 10% (w/v) polyethylene glycol 4000, 0.2 M MgCl₂, 60 mM K₂SO₄, 0.1 M MES buffer and pH 6.5 for the tetragonal crystals. The protein was crystallised in the presence of the co-substrate NADP⁺.

Oil and oil with addition of 2,3-butanediol were used as cryo-condition prior to flash freezing the crystals in liquid nitrogen for the tetragonal and orthorhombic crystal, respectively. X-ray diffraction data sets of the two CtADH crystals were collected at beamline ID23-1 of the European Synchrotron

Radiation Facility (ESRF) in Grenoble, France, using a wavelength of 0.97970 Å (orthorhombic CtADH crystal) and at beamline PXIII of the Swiss Light Source (SLS) in Villigen, Switzerland, using a wavelength of 1.00000 Å (tetragonal CtADH crystal). The data collection temperature was 100 K. The data were processed with the AUTOPROC toolbox (version 1.0.5, Global Phasing Limited, Cambridge, UK) using default settings [42]. The pipeline applied XDS (BUILT 20200417) [43] for indexing and integration, POINTLESS (version 1.11.21) [44] and AIMLESS (version 0.7.4) [45] from the CCP4 suite (version 7.1.000) [46] for space group determination and scaling and finally STARANISO (version 2.3.36) [47] for anisotropy analysis.

The CtADH structures were solved with molecular replacement using PHASER (version 2.8.3) [48] within PHENIX (version 1.18.2-3874) [49] and the SyADH structure PDB-ID 4BMV [26] as search model. The structures were optimized with several rounds of PHENIX refinement [49] followed by manual modelling with COOT (version 0.9) [50] and deposited at the PDB with the codes 6ZE0 (orthorhombic structure) and 6ZDZ (tetragonal structure). The illustrations in Figure 3 were prepared with PYMOL, version 1.7.0.3 [51].

3.5. Enzyme Activity Assays

Assays for ADH activity were performed spectrophotometrically by measuring the consumption of the cofactor NADPH. The standard assay was performed in 100 mM citrate-phosphate buffer at a pH value of 6.0 with 10 mM propiophenone (unless otherwise stated). The specific activity of the purified CtADH (0.1 mg/mL) was determined for various substrates in concentrations between 1 and 50 mM in 100 mM citrate-phosphate buffer (pH 6.0) with 0.2 mM NADPH for reductions and 0.2 mM NADP⁺ for oxidations, respectively. All spectrophotometric measurements were performed at least in triplicates.

Additionally, the K_M -values for the substrates propiophenone and phenyl-1-ethanol as well as for the cofactor NADP(H) were determined. All measurements were carried out in a total volume of 300 µL in microtiter plates. In 100 mM citrate-phosphate buffer, pH 6.0, containing propiophenone (0.01 mM–13.59 mM) purified CtADH with a concentration of 0.13 mg/mL was added. For phenyl-1-ethanol (0.01 mM–12.96 mM), 0.25 mg/mL of purified enzyme was added. The specific activity was determined after adding NADPH (0.36 mM) for propiophenone and phenyl-1-ethanol through measuring the change of absorbance at 340 nm over 1 min at different temperatures (propiophenone 27.4 °C, phenyl-1-ethanol 29.4 °C) using a Tecan Reader. The K_M -values of NADP⁺ and NADPH (0.01 mM–0.35 mM) were determined measuring the specific activity of CtADH with propiophenone as substrate at a fixed concentration of 2 mM at 27.5 °C for NADP⁺ and 28.8 °C for NADPH with 0.1 mg/mL purified CtADH.

3.6. Effect of Organic Solvents and pH on the Stability and Activity of CtADH

The effect of various organic solvents (methanol, ethanol, isopropanol, dimethyl sulfoxide (DMSO), ethyl acetate, dichloromethane, acetonitrile, toluene, methyl tert-butyl ether (MTBE)) on the stability of purified CtADH was evaluated by incubating the enzyme with either 10, 25 or 50% (*v/v*) of the specified organic solvent at 22 °C for 2 h. For the water-soluble solvents, the samples were shaken at 1000 rpm, and for the water insoluble solvents, they were inverted with 13 rpm with a laboratory rotator from IKA (Loopster basic). The CtADH activity was then assayed using propiophenone (10 mM) as substrate in 100 mM citrate-phosphate buffer, pH 6, at 25 °C. Relative activity was calculated based on a control in which buffer was added instead of the organic solvent. To evaluate the pH-profile of CtADH, the enzyme solution was diluted in different buffers, covering a broad pH range, and incubated for 10 min at room temperature. Details are described in chapter 6.2 of the Supporting Information. All spectrophotometric measurements were performed at least in triplicates.

3.7. Determination of the Enantioselectivity

The enantioselectivity of CtADH in the reduction of different ketones was examined with the use of D-glucose and a modified heat purified glucose dehydrogenase (GDH) from *Bacillus subtilis* to achieve continuous NADPH recycling [52]. The different biotransformations were performed as

follows: 10 mM substrate, 20 mM D-glucose, 0,2 mM NADP⁺, 3 U GDH, 10 mg purified CtADH in a final volume of 1.5 mL 100 mM citrate-phosphate buffer, pH 6.0, incubated at 30 °C. After 2 h, the reaction mixture was extracted with ethyl acetate (3 mL) and analysed by chiral GC (Shimadzu GC-2010 Plus). The experimental details of the GC analyses and the measured retention times are given in chapter 7 of the Supporting Information.

4. Conclusions

In this study, we report the *in silico* identification, cloning, heterologous expression and functional as well as structural characterization of an NADPH-dependent alcohol dehydrogenase from *C. testosteroni* (CtADH). The enzyme displays a wide pH tolerance and a broad substrate range including bulky–bulky ketones and is, thus, particularly attractive for applications as a biocatalyst in the context of sustainable biotechnology. Furthermore, CtADH shows an excellent enantioselectivity to (S)-alcohols, which makes it a suitable candidate as a biocatalyst for the production of chiral building blocks. The CtADH crystal structures of this work allow a basic understanding of the enzyme's bulky–bulky substrate profile. In conclusion, this work emphasizes that *in silico* screening to identify novel enzymes with desired characteristics is a good alternative to complex and expensive mutagenesis studies.

Supplementary Materials: The following are available online at <http://www.mdpi.com/2073-4344/10/11/1281/s1>, 1. Cloned sequence of alcohol dehydrogenase from *Comamonas testosteroni* (DSM 38). 2. Molecular cloning of CtADH. 3. Preparation of crude extract. 4. Figure S1: SDS-Page analysis of protein expression of CtADH in *E. coli* BL21(DE3) with different conditions (a) and SDS-Page gel picture from purification of CtADH. 5. Table S1: X-ray diffractometry. 6. Enzyme assays; Figure S2: Michaelis–Menten diagrams of CtADH towards propiophenone and NADPH (reduction) as well as (S)-phenylethanol (oxidation). 7. Analytical methods; Table S3: List of used GC-methods; Table S4: List of measured retention times. 8. Figure S3: Thermal shift assay of CtADH.

Author Contributions: Conceptualization, W.H., H.G., D.B. and C.T.; methodology: D.B., M.S., C.T. and K.N.; supervision, H.G., K.N. and W.H.; funding acquisition: K.N., W.H. and H.G.; writing: D.B., C.T., M.S., K.N. and H.G. All authors have read and agreed to the published version of the manuscript.

Funding: The work was funded by the Deutsche Forschungsgemeinschaft (DFG; project B07 of SFB635) as well as the Bundesministerium für Bildung und Forschung within the funding programme “Biotechnologie 2020+, Nächste Generation biotechnologischer Verfahren” (BMBF; Grant No. 031A184A).

Acknowledgments: We thank Marco Drexelius for crystallization support with CtADH and the staff of the beamlines ID23-1 (ESRF, Grenoble, France) and PXIII (SLS, Villigen, Switzerland) for assistance with X-ray diffraction data collection. We are particularly grateful to Professor Ulrich Baumann (University of Cologne) for access to protein crystallography infrastructure and continuous support. Furthermore, we acknowledge support for the publication costs from the Open Access Publication Fund of Bielefeld University.

Conflicts of Interest: The authors declare no conflict of interest.

References

1. Bulut, D.; Duangdee, N.; Gröger, H.; Berkessel, A.; Hummel, W.; Groeger, H. Screening, Molecular Cloning, and Biochemical Characterization of an Alcohol Dehydrogenase from *Pichia pastoris* Useful for the Kinetic Resolution of a Racemic β -Hydroxy- β -trifluoromethyl Ketone. *ChemBioChem* **2016**, *17*, 1349–1358. [[CrossRef](#)] [[PubMed](#)]
2. Gröger, H.; Chamouleau, F.; Orologas, N.; Rollmann, C.; Drauz, K.; Hummel, W.; Weckbecker, A.; May, O. Enantioselective Reduction of Ketones with “Designer Cells” at High Substrate Concentrations: Highly Efficient Access to Functionalized Optically Active Alcohols. *Angew. Chem. Int. Ed.* **2006**, *45*, 5677–5681. [[CrossRef](#)] [[PubMed](#)]
3. Woodyer, R.; Wheatley, J.L.; Relyea, H.A.; Rimkus, S.; Van Der Donk, W.A. Site-Directed Mutagenesis of Active Site Residues of Phosphite Dehydrogenase. *Biochemistry* **2005**, *44*, 4765–4774. [[CrossRef](#)] [[PubMed](#)]
4. Gröger, H.; Zumbrägel, N.; Wetzl, D.; Iding, H. Asymmetric Biocatalytic Reduction of Cyclic Imines: Design and Application of a Tailor-Made Whole-Cell Catalyst. *Heterocycles* **2017**, *95*, 1261. [[CrossRef](#)]
5. Ni, Y.; Holtmann, D.; Hollmann, F. How green is biocatalysis? To calculate is to know. *ChemCatChem* **2014**, *6*, 930–943. [[CrossRef](#)]

6. Dennig, A.; Blaschke, F.; Gandomkar, S.; Tassano, E.; Nidetzky, B. Preparative Asymmetric Synthesis of Canonical and Non-canonical α -amino Acids Through Formal Enantioselective Biocatalytic Amination of Carboxylic Acids. *Adv. Synth. Catal.* **2019**, *361*, 1348–1358. [[CrossRef](#)]
7. Zhu, Y.-H.; Liu, C.-Y.; Cai, S.; Guo, L.-B.; Kim, I.-W.; Kalia, V.C.; Lee, J.-K.; Zhang, Y.-W. Cloning, Expression and Characterization of a Highly Active Alcohol Dehydrogenase for Production of Ethyl (S)-4-Chloro-3-Hydroxybutyrate. *Indian J. Microbiol.* **2019**, *59*, 225–233. [[CrossRef](#)] [[PubMed](#)]
8. Che, Y.; Yin, S.; Wang, H.; Yang, H.; Xu, R.; Wang, Q.; Wu, Y.; Boutet, J.; Huet, R.; Wang, C. Production of Methionol from 3-Methylthiopropionaldehyde by Catalysis of the Yeast Alcohol Dehydrogenase Adh4p. *J. Agric. Food Chem.* **2020**, *68*, 4650–4656. [[CrossRef](#)]
9. Kallberg, Y.; Oppermann, U.; Jörnvall, H.; Persson, B. Short-chain dehydrogenase/reductase (SDR) relationships: A large family with eight clusters common to human, animal, and plant genomes. *Protein Sci.* **2009**, *11*, 636–641. [[CrossRef](#)]
10. Hummel, W.; Gröger, H. Strategies for regeneration of nicotinamide coenzymes emphasizing self-sufficient closed-loop recycling systems. *J. Biotechnol.* **2014**, *191*, 22–31. [[CrossRef](#)]
11. Weckbecker, A.; Gröger, H.; Hummel, W. Regeneration of Nicotinamide Coenzymes: Principles and Applications for the Synthesis of Chiral Compounds. *Biosyst. Eng. I* **2010**, *120*, 195–242. [[CrossRef](#)]
12. Weckbecker, A.; Hummel, W. *Glucose Dehydrogenase for the Regeneration of NADPH and NADH*; Barredo, J.L., Ed.; Humana Press: Totawa, NJ, USA, 2005; pp. 225–238.
13. Schlieben, N.H.; Niefind, K.; Müller, J.; Riebel, B.; Hummel, W.; Schomburg, D. Atomic Resolution Structures of R-specific Alcohol Dehydrogenase from *Lactobacillus brevis* Provide the Structural Bases of its Substrate and Cosubstrate Specificity. *J. Mol. Biol.* **2005**, *349*, 801–813. [[CrossRef](#)]
14. Machielsen, R.; Uria, A.R.; Kengen, S.W.M.; Van Der Oost, J. Production and Characterization of a Thermostable Alcohol Dehydrogenase That Belongs to the Aldo-Keto Reductase Superfamily. *Appl. Environ. Microbiol.* **2006**, *72*, 233–238. [[CrossRef](#)]
15. Petratos, K.; Gessmann, R.; Daskalakis, V.; Papadovasilaki, M.; Papanikolaou, Y.; Tsigos, I.; Bouriotis, V. Structure and Dynamics of a Thermostable Alcohol Dehydrogenase from the Antarctic Psychrophile *Moraxella* sp. TAE123. *ACS Omega* **2020**, *5*, 14523–14534. [[CrossRef](#)] [[PubMed](#)]
16. Lavandera, I.; Kern, A.; Schaffenberger, M.; Gross, J.; Glieder, A.; De Wildeman, S.; Kroutil, W. An Exceptionally DMSO-Tolerant Alcohol Dehydrogenase for the Stereoselective Reduction of Ketones. *ChemSusChem* **2008**, *1*, 431–436. [[CrossRef](#)]
17. Lavandera, I.; Kern, A.; Resch, V.; Ferreira-Silva, B.; Glieder, A.; Fabian, W.M.F.; De Wildeman, S.; Kroutil, W. One-Way Biohydrogen Transfer for Oxidation of *sec*-Alcohols. *Org. Lett.* **2008**, *10*, 2155–2158. [[CrossRef](#)]
18. Hu, J.; Li, G.; Liang, C.; Shams, S.; Zhu, S.; Zheng, G. Stereoselective synthesis of the key intermediate of ticagrelor and its diverse analogs using a new alcohol dehydrogenase from *Rhodococcus kyotonensis*. *Process Biochem.* **2020**, *92*, 232–243. [[CrossRef](#)]
19. Horinouchi, M.; Hayashi, T.; Kudo, T. Steroid degradation in *Comamonas testosteroni*. *J. Steroid Biochem. Mol. Biol.* **2012**, *129*, 4–14. [[CrossRef](#)] [[PubMed](#)]
20. Horinouchi, M.; Kurita, T.; Hayashi, T.; Kudo, T. Steroid degradation genes in *Comamonas testosteroni* TA441: Isolation of genes encoding a $\Delta 4(5)$ -isomerase and 3α - and 3β -dehydrogenases and evidence for a 100kb steroid degradation gene hot spot. *J. Steroid Biochem. Mol. Biol.* **2010**, *122*, 253–263. [[CrossRef](#)]
21. Wang, L.-J.; Li, C.-X.; Ni, Y.; Zhang, J.; Liu, X.; Xu, J.-H. Highly efficient synthesis of chiral alcohols with a novel NADH-dependent reductase from *Streptomyces coelicolor*. *Bioresour. Technol.* **2011**, *102*, 7023–7028. [[CrossRef](#)] [[PubMed](#)]
22. Niefind, K.; Müller, J.; Riebel, B.; Hummel, W.; Schomburg, I. The crystal structure of R-specific alcohol dehydrogenase from *Lactobacillus brevis* suggests the structural basis of its metal dependency. *J. Mol. Biol.* **2003**, *327*, 317–328. [[CrossRef](#)]
23. Lavandera, I.; Kern, A.; Ferreira-Silva, B.; Glieder, A.; De Wildeman, S.; Kroutil, W. Stereoselective Bioreduction of Bulky-Bulky Ketones by a Novel ADH from *Ralstonia* sp. *J. Org. Chem.* **2008**, *73*, 6003–6005. [[CrossRef](#)] [[PubMed](#)]
24. Kulig, J.; Frese, A.; Kroutil, W.; Pohl, M.; Rother, D. Biochemical characterization of an alcohol dehydrogenase from *Ralstonia* sp. *Biotechnol. Bioeng.* **2013**, *110*, 1838–1848. [[CrossRef](#)]
25. Lavandera, I.; Oberdorfer, G.; Gross, J.; De Wildeman, S.; Kroutil, W. Stereocomplementary Asymmetric Reduction of Bulky–Bulky Ketones by Biocatalytic Hydrogen Transfer. *Eur. J. Org. Chem.* **2008**, *2008*, 2539–2543. [[CrossRef](#)]

26. Man, H.; Kedziora, K.W.; Kulig, J.K.; Frank, A.; Lavandera, I.; Gotor-Fernández, V.; Rother, D.; Hart, S.; Turkenburg, J.P.; Grogan, G. Structures of Alcohol Dehydrogenases from *Ralstonia* and *Sphingobium* spp. Reveal the Molecular Basis for Their Recognition of 'Bulky–Bulky' Ketones. *Top. Catal.* **2013**, *57*, 356–365. [[CrossRef](#)]
27. Chen, Y.-L.; Wang, C.-H.; Yang, F.-C.; Ismail, W.; Wang, P.-H.; Shih, C.-J.; Wu, Y.-C.; Chiang, Y.-R. Identification of *Comamonas testosteroni* as an androgen degrader in sewage. *Sci. Rep.* **2016**, *6*, 35386. [[CrossRef](#)] [[PubMed](#)]
28. Fukuda, K.; Hosoyama, A.; Tsuchikane, K.; Ohji, S.; Yamazoe, A.; Fujita, N.; Shintani, M.; Kimbara, K. Complete Genome Sequence of Polychlorinated Biphenyl Degradator *Comamonas testosteroni* TK102 (NBRC 109938). *Genome Announc.* **2014**, *2*. [[CrossRef](#)] [[PubMed](#)]
29. Ma, Y.-F.; Zhang, Y.; Zhang, J.-Y.; Chen, D.; Zhu, Y.; Zheng, H.; Wang, S.-Y.; Jiang, C.-Y.; Zhao, G.-P.; Liu, S.-J. The Complete Genome of *Comamonas testosteroni* Reveals Its Genetic Adaptations to Changing Environments. *Appl. Environ. Microbiol.* **2009**, *75*, 6812–6819. [[CrossRef](#)]
30. Liu, L.; Zhu, W.; Cao, Z.; Xu, B.; Wang, G.; Wang, G. High correlation between genotypes and phenotypes of environmental bacteria *Comamonas testosteroni* strains. *BMC Genom.* **2015**, *16*, 110. [[CrossRef](#)]
31. Liu, C.; Liu, K.; Zhao, C.; Gong, P.; Yu, Y. The characterization of a short chain dehydrogenase/reductase (SDRx) in *Comamonas testosteroni*. *Toxicol. Rep.* **2020**, *7*, 460–467. [[CrossRef](#)]
32. Liu, L.; Jiang, C.; Liu, X.-Y.; Wu, J.-F.; Han, J.-G.; Liu, S.-J. Plant-microbe association for rhizoremediation of chloronitroaromatic pollutants with *Comamonas* sp. strain CNB-1. *Environ. Microbiol.* **2007**, *9*, 465–473. [[CrossRef](#)]
33. Loffhagen, N.; Babel, W. Energization of *Comamonas testosteroni* ATCC 17454 for Indicating Toxic Effects of Chlorophenoxy Herbicides. *Arch. Environ. Contam. Toxicol.* **2003**, *45*, 317–323. [[CrossRef](#)]
34. Benson, D.A.; Clark, K.; Karsch-Mizrachi, I.; Lipman, D.J.; Ostell, J.; Sayers, E.W. GenBank. *Nucleic Acids Res.* **2014**, *41*, D36–D42. [[CrossRef](#)] [[PubMed](#)]
35. Robert, X.; Gouet, P. Deciphering key features in protein structures with the new ENDscript server. *Nucleic Acids Res.* **2014**, *42*, W320–W324. [[CrossRef](#)] [[PubMed](#)]
36. De Miranda, A.S.; Simon, R.C.; Grischek, B.; De Paula, G.C.; Horta, B.A.C.; De Miranda, L.S.M.; Kroutil, W.; Kappe, C.O.; De Souza, R.O.M.A. Chiral Chlorohydrins from the Biocatalyzed Reduction of Chloroketones: Chiral Building Blocks for Antiretroviral Drugs. *ChemCatChem* **2015**, *7*, 984–992. [[CrossRef](#)]
37. Yang, Z.-Y.; Ye, W.-J.; Xie, Y.-Y.; Liu, Q.-H.; Chen, R.; Wang, H.-L.; Wei, D.-Z. Efficient Asymmetric Synthesis of Ethyl (S)-4-Chloro-3-hydroxybutyrate Using Alcohol Dehydrogenase SmADH31 with High Tolerance of Substrate and Product in a Monophasic Aqueous System. *Org. Process Res. Dev.* **2020**, *24*, 1068–1076. [[CrossRef](#)]
38. Liu, Z.-Q.; Dong, S.-C.; Yin, H.-H.; Xue, Y.; Tang, X.-L.; Zhang, X.-J.; He, J.-Y.; Zheng, Y.-G. Enzymatic synthesis of an ezetimibe intermediate using carbonyl reductase coupled with glucose dehydrogenase in an aqueous-organic solvent system. *Bioresour. Technol.* **2017**, *229*, 26–32. [[CrossRef](#)] [[PubMed](#)]
39. Reetz, M.T. Biocatalysis in Organic Chemistry and Biotechnology: Past, Present, and Future. *J. Am. Chem. Soc.* **2013**, *135*, 12480–12496. [[CrossRef](#)]
40. Riebel, B. Biochemische und molekularbiologische Charakterisierung neuer mikrobieller NAD(P)-abhängiger Alkoholdehydrogenasen. Ph.D. Thesis, Heinrich-Heine-Universität Düsseldorf, Düsseldorf, Germany, 1996.
41. Altschul, S.F.; Madden, T.L.; Schäffer, A.A.; Zhang, J.; Zhang, Z.; Miller, W.; Lipman, D.J. Gapped BLAST and PSI-BLAST: A new generation of protein database search programs. *Nucleic Acids Res.* **1997**, *25*, 3389–3402. [[CrossRef](#)]
42. Vonnrhein, C.; Flensburg, C.; Keller, P.; Sharff, A.; Smart, O.; Paciorek, W.; Womack, T.; Bricogne, G. Data processing and analysis with the autoPROC toolbox. *Acta Crystallogr. D Biol. Crystallogr.* **2011**, *67*, 293–302. [[CrossRef](#)]
43. Kabsch, W. XDS. *Acta Crystallogr. D Biol. Crystallogr.* **2010**, *66*, 125–132. [[CrossRef](#)]
44. Evans, P.R. Scaling and assessment of data quality. *Acta Crystallogr. Sect. D Biol. Crystallogr.* **2005**, *62*, 72–82. [[CrossRef](#)]
45. Evans, P.R.; Murshudov, G.N. How good are my data and what is the resolution? *Acta Crystallogr. Sect. D Biol. Crystallogr.* **2013**, *69*, 1204–1214. [[CrossRef](#)]
46. Winn, M.D.; Ballard, C.C.; Cowtan, K.D.; Dodson, E.J.; Emsley, P.; Evans, P.R.; Keegan, R.M.; Krissinel, E.B.; Leslie, A.G.W.; McCoy, A.; et al. Overview of the CCP4 suite and current developments. *Acta Crystallogr. Sect. D Biol. Crystallogr.* **2011**, *67*, 235–242. [[CrossRef](#)]
47. Tickle, I.J.; Flensburg, C.; Keller, P.; Paciorek, W.; Sharff, A.; Vonnrhein, C.; Bricogne, G. STARANISO; Global Phasing Ltd.: Cambridge, UK, 2018.

48. McCoy, A.J.; Grosse-Kunstleve, R.W.; Adams, P.D.; Winn, M.D.; Storoni, L.C.; Read, R.J. Phaser crystallographic software. *J. Appl. Crystallogr.* **2007**, *40*, 658–674. [[CrossRef](#)] [[PubMed](#)]
49. Adams, P.D.; Afonine, P.V.; Bunkóczi, G.; Chen, V.B.; Davis, I.W.; Echols, N.; Headd, J.J.; Hung, L.-W.; Kapral, G.J.; Grosse-Kunstleve, R.W.; et al. PHENIX: A comprehensive Python-based system for macromolecular structure solution. *Acta Crystallogr. Sect. D Biol. Crystallogr.* **2010**, *66*, 213–221. [[CrossRef](#)]
50. Emsley, P.; Lohkamp, B.; Scott, W.G.; Cowtan, K. Features and development of Coot. *Acta Crystallogr. Sect. D Biol. Crystallogr.* **2010**, *66*, 486–501. [[CrossRef](#)] [[PubMed](#)]
51. *The PyMOL Molecular Graphics System*, version 1.7.0.3; Schrödinger, LLC: New York, NY, USA, 2012.
52. Vázquez-Figueroa, E.; Chaparro-Riggers, J.; Bommarius, A.S. Development of a Thermostable Glucose Dehydrogenase by a Structure-Guided Consensus Concept. *ChemBioChem* **2007**, *8*, 2295–2301. [[CrossRef](#)]

Publisher’s Note: MDPI stays neutral with regard to jurisdictional claims in published maps and institutional affiliations.



© 2020 by the authors. Licensee MDPI, Basel, Switzerland. This article is an open access article distributed under the terms and conditions of the Creative Commons Attribution (CC BY) license (<http://creativecommons.org/licenses/by/4.0/>).